

GPU Graph Processing on CXL-Based Microsecond-Latency External Memory

Shintaro Sano, Yosuke Bando, Kazuhiro Hiwada, Hirotsugu Kajihara, Tomoya Suzuki,
Yu Nakanishi, Daisuke Taki, Akiyuki Kaneko, Tatsuo Shiozawa
{shintarou.sano,yosuke1.bando,kazuhiro.hiwada,hirotsugu.kajihara,tomoya.suzuki}@kioxia.com
{yu.nakanishi,daisuke.taki,akiyuki.kaneko,tatsuo.shiozawa}@kioxia.com
Kioxia Corporation
Japan

ABSTRACT

In GPU graph analytics, the use of external memory such as the host DRAM and solid-state drives is a cost-effective approach to processing large graphs beyond the capacity of the GPU onboard memory. This paper studies the use of Compute Express Link (CXL) memory as alternative external memory for GPU graph processing in order to see if this emerging memory expansion technology enables graph processing that is as fast as using the host DRAM. Through analysis and evaluation using FPGA prototypes, we show that representative GPU graph traversal algorithms involving fine-grained random access can tolerate an external memory latency of up to a few microseconds introduced by the CXL interface as well as by the underlying memory devices. This insight indicates that microsecond-latency flash memory may be used as CXL memory devices to realize even more cost-effective GPU graph processing while still achieving performance close to using the host DRAM.

CCS CONCEPTS

• **Hardware** → **Analysis and design of emerging devices and systems; Memory and dense storage.**

KEYWORDS

CXL, memory, flash, GPU, graph, latency

ACM Reference Format:

Shintaro Sano, Yosuke Bando, Kazuhiro Hiwada, Hirotsugu Kajihara, Tomoya Suzuki, Yu Nakanishi, Daisuke Taki, Akiyuki Kaneko, Tatsuo Shiozawa. 2023. GPU Graph Processing on CXL-Based Microsecond-Latency External Memory. In *Workshops of The International Conference on High Performance Computing, Network, Storage, and Analysis (SC-W 2023)*, November 12–17, 2023, Denver, CO, USA. ACM, New York, NY, USA, 11 pages. <https://doi.org/10.1145/3624062.3624173>

1 INTRODUCTION

Graphics processing units (GPUs) have become one of the most commonly-used accelerators in high-performance computing and machine learning. In order to handle ever-growing data sizes in these applications beyond the relatively limited capacity (tens of GBs) of GPU onboard memory, the use of external memory such as

the host DRAM and solid-state drives (SSDs) can be a cost-effective approach compared with pooling multiple GPUs' memory together [9–11, 18, 22, 28, 31, 33, 37, 39, 40, 43]. In particular, GPU-centric external memory access methods have been shown to yield the state-of-the-art runtime performance in workloads involving on-demand, fine-grained random access such as graph analytics [31, 33]. That is, when small pieces of data to be read next depend on the current processing results and cannot be *a priori* determined, it is more efficient to have the GPU initiate data requests than to have the CPU control the data flow between the GPU and external memory.

In GPU-initiated data access in graph analytics, the use of the host DRAM generally leads to faster processing speeds than SSDs (see Sections 2.2 and 4.1.2 for details). However, increasing the host DRAM capacity to accommodate large graph data can be costly. Memory expansion via Compute Express Link (CXL) [4] is a promising alternative, as it allows load/store access to pooled memory in a cache-coherent manner over more expandable PCIe links. That being said, CXL memory introduces additional latency to the underlying memory devices (e.g., DRAM), and an added latency of one or two hundred *nanoseconds* is shown to already have an adverse performance impact on some of CPU-based workloads [23].

In this paper, we are concerned about the use of CXL memory as external memory for GPU graph processing in order to see if this emerging memory expansion technology enables graph processing that is as fast as using the host DRAM. The question we are interested in is whether GPU graph processing is tolerant to longer latency CXL introduces, and, if so, how much longer. The latter part of the question is because, if the allowable latency is longer than the DRAM-based CXL memory latency, less expensive memory devices including low-latency flash memory may be used in place of DRAM. In fact, our analysis indicates that, as opposed to the case of CPU workloads mentioned above, representative GPU graph traversal algorithms are latency-tolerant thanks to their massive parallelism. The bottleneck comes from the PCIe link, which still leaves a permissible latency of a few *microseconds*.

In order to back up our analysis at this early stage of CXL deployment when supporting devices are limited in availability, we use two FPGA prototypes. The first prototype is equipped with microsecond-latency flash memory, and works as a PCIe-attached storage device [38]. While it does not support the CXL interface, it nonetheless supports access at a smaller address alignment size than the standard minimum unit of 512 bytes in Non-Volatile Memory Express (NVMe) SSDs, in order to serve fine-grained random read requests in graph workloads. The second prototype is DRAM-based CXL memory, which we implement based on Intel Agilix[®]7 FPGA

SC-W 2023, November 12–17, 2023, Denver, CO, USA

© 2023 Copyright held by the owner/author(s). Publication rights licensed to ACM. This is the author's version of the work. It is posted here for your personal use. Not for redistribution. The definitive Version of Record was published in *Workshops of The International Conference on High Performance Computing, Network, Storage, and Analysis (SC-W 2023)*, November 12–17, 2023, Denver, CO, USA, <https://doi.org/10.1145/3624062.3624173>.

supporting the CXL interface. Our FPGA design features adjustable latency for the onboard DRAM, allowing us to evaluate CXL memory with longer latency. Using the first prototype, we show that external memory having high random read performance backed by low-latency flash memory allows us to approach host DRAM-based GPU graph processing speeds, if it supports a small address alignment size. This also confirms that the address alignment size is the primary performance factor that sets the host DRAM-based method apart from the SSD-based method, supporting the potential of CXL-based external memory that can be accessed in the same way as the host DRAM. Using the second prototype supporting the CXL interface and allowing the same GPU code to work with the host DRAM and CXL memory, we show that the runtimes on the host DRAM and CXL memory are almost identical as long as the CXL memory latency is under a certain allowable value. To the best of our knowledge, evaluation of GPU graph processing on CXL memory has not been reported before.

In summary, our contributions are:

- We show that the performance of GPU graph processing is lenient to external memory latency, and a few microseconds may be tolerated in achieving processing speeds comparable to using the host DRAM.
- Using an FPGA-based external memory device equipped with microsecond-latency flash memory, we demonstrate GPU graph processing speeds close to using the host DRAM, confirming the importance of small address alignments, which also applies to when the GPU accesses CXL memory.
- Using another FPGA device implementing CXL memory with adjustable latency, we evaluate GPU graph processing on CXL memory for the first time, and confirm that the same GPU code runs as fast as when using the host DRAM as long as the CXL memory latency is up to a few microseconds.

2 PRELIMINARIES

This section provides background information by explaining graph traversal on external memory, defining our performance metric, and then briefly reviewing how CPU graph traversal on low-latency flash memory was made as fast as that on the host DRAM.

2.1 Graph Traversal on External Memory

A graph is represented in the commonly-used compressed sparse row (CSR) format consisting of a vertex list and an edge list as shown in Figure 1. Suppose Vertex 1 points to five vertices as shown in the right-hand side of the figure. The IDs of those five vertices appear in a contiguous subset of the edge list (called a *sublist* in this paper). The start and end (exclusive) indices of this sublist is stored at Vertices 1 and 2 in the vertex list. Since the number of edges is an order of magnitude larger than that of vertices as in Table 1, the edge list is stored on the external memory. When a graph is traversed, an edge sublist is read from external memory, whose size depends on the vertex’s degree, which is typically a few hundred bytes on average [31] as observed in Table 1. Since vertices in this sublist determines next edge sublists to be read, access is fine-grained, random, and on-demand (cannot be determined beforehand).

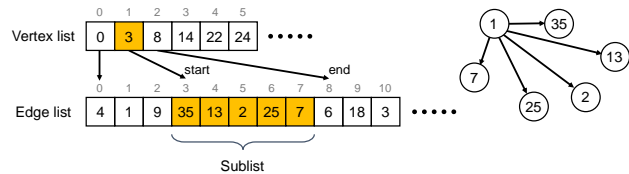


Figure 1: Compressed Sparse Row (CSR) format example.

Table 1: Graph datasets.

Dataset	Num. of vertices	Num. of edges (edge list size)	Ave. degrees* (sublist size)
urand27 [2]	134 mil.	4.4 bil. (35.2 GB)	32.0 (256.0 B)
kron27 [2]	134 mil.	4.2 bil. (33.6 GB)	67.0 (536.0 B)
Friendster [45]	125 mil.	3.6 bil. (28.8 GB)	55.1 (440.8 B)

* 8 bytes per vertex ID. 0-degree vertices are excluded from the average.

2.2 Processing Time as Performance Metric

As mentioned in Section 1, the host DRAM-based method EMOGI [31] is generally faster than the SSD-based method BaM [33] in terms of *graph processing time*. If EMOGI’s runtime includes the time for loading graph data onto the host DRAM from the SSDs (data loading time) in addition to the time for running the algorithm on the GPU (graph processing time), BaM is shown to be competitive for some benchmark workloads. However, in real-world applications where one might perform more complex graph analytics, the data loading time can be negligible, making the graph processing time dominant. Moreover, since we are interested in the use of non-volatile memory, graph data may be stored on CXL memory from the beginning without loading from SSDs. Thus, we use graph processing time alone as a performance metric in this paper.

2.3 Review of CPU Graph Processing Case

In CPU graph processing, it has previously been shown that, using microsecond-latency flash memory as external memory, processing speeds can be close to when using the host DRAM [42]. As multiple dies of microsecond-latency flash memory can support sufficient random read performance required for in-memory-class graph processing, naive external memory execution slows down not due to random read performance (in input/output operations per second, or IOPS) of the external memory, but due to the longer latency of external memory and the CPU overhead of issuing a large number of read requests. These issues are overcome by using lightweight context switching to hide the latency and a lightweight storage access method to reduce the CPU overhead.

3 ANALYSIS

This section characterizes the performance of GPU graph processing in terms of how the GPU accesses edge data.

The performance characteristics of GPU graph processing is different from the CPU case reviewed in Section 2.3. The difference comes from massively parallel compute resources available on the GPU and the relatively limited bandwidth of the PCIe link to the

GPU. This puts the bottleneck on the PCIe link. In fact, both of the state-of-the-art GPU graph processing methods EMOGI (based on the host DRAM) and BaM (SSDs) achieve a data transfer rate close to the peak PCIe bandwidth. Therefore, the performance is primarily determined by how the PCIe bandwidth to the GPU is utilized effectively.

To examine this, we look at the runtime t of a given graph traversal task for a given graph dataset in terms of how fast the GPU consumes data through the PCIe link, as

$$t = \frac{D}{T} \quad (1)$$

where D is the total data size to be read from external memory to complete the task, and T is the average data throughput (in MB/sec) to the GPU. Obviously, we would like to decrease D and increase T for faster execution.

Using this equation, our analysis proceeds as follows. Ideally, the best performance is obtained when D is equal to the sum E of the edge sublist sizes needed to be accessed to complete the task, and when T hits the PCIe bandwidth W . However, external memory access is done in units of a certain address alignment size coming from hardware and cache implementations, which amplifies the total data size D . We will see how this amplification behaves as a function of address alignment size a in Section 3.1, while the throughput T will be modeled in Section 3.2. Once Equation 1 is characterized, Section 3.3 revisits existing methods EMOGI and BaM in light of Equation 1. As will be described in Section 3.4, this revisit suggests opportunities for low-latency memory devices to be a cost-effective alternative to the host DRAM and be more performant than standard SSDs when used as external memory for GPU graph processing. In Section 3.5, we confirm that the microsecond latency allowance coming from the PCIe bottleneck is unlikely to be limited by other factors.

3.1 Read Amplification

When edge sublists are read from external memory at a certain address alignment size a , fetched data may contain some unused part of the edge list. For example, Figure 2 shows the situation where $3a$ bytes need to be read in order to fetch Edge sublist 1. Suppose the current graph traversal step requires Sublists 1 and 2 but not 3. Then, after reading the $3a$ bytes, Sublist 2 is likely to be on the GPU cache, but the $3a$ bytes still contain part of Sublist 3 that will not be used soon (and may be evicted from the cache before it is referenced later). Therefore, the ratio of the fetched data to the data actually used, D/E , is generally greater than one. We refer to this ratio as *read amplification factor*, or RAF. In general, smaller alignments are better at reducing the RAF, given the small average edge sublist size of a few hundred bytes in graph processing.

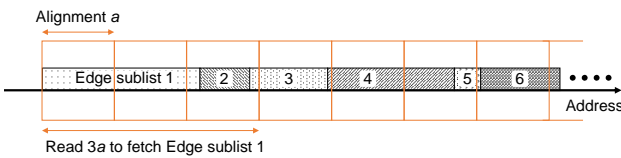


Figure 2: Aligned reads of edge sublists.

To illustrate this, we ran representative graph traversal algorithms involving fine-grained random access, breadth first search (BFS) and single-source shortest path (SSSP), for varying alignment sizes and calculated the RAF. This is CPU simulation implementing a software cache to experiment with alignment sizes without hardware constraints, but we confirmed that our RAF evaluation of BFS with 512 B and 4 kB alignments match the BaM measurements well. Figure 3 shows RAF values for the three graph datasets in Table 1. As shown, the RAFs are increasing functions of the alignment size, which can be up to 4 at 4 kB.

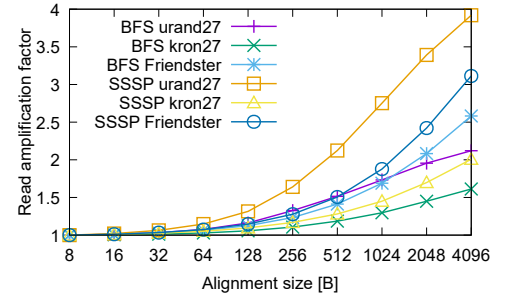


Figure 3: Read amplification for varying alignment size.

3.2 Throughput

Here we examine the denominator of Equation 1. The throughput can be modeled by the following equation.

$$T = \min \left\{ Sd, \frac{N_{\max}}{L} d, W \right\}, \quad (2)$$

where d is the average data transfer size per read request, S is the random read performance in IOPS of the external memory, L is the average latency (including latencies of the PCIe link, CXL interface, and memory devices), N_{\max} is the maximum number of outstanding (in other words, in-flight or concurrent) requests that can be issued through the PCIe link, and W is the PCIe bandwidth. The first term in the min operation trivially states that the throughput is the product of the IOPS and the data size per IO, but it is capped by the PCIe bandwidth W in the third term. The second term introduces an additional limit imposed by Little's Law stating that (by adapting it to our case) the data size passing through the link at any given time instance (N concurrent data transfers of size d) is equal to the product of the throughput and latency:

$$Nd = TL. \quad (3)$$

This means that the throughput is capped as $T = Nd/L \leq N_{\max} d/L$. Note that this limit by PCIe is imposed for memory (host DRAM or CXL) access but not for storage access. In the storage case, the limit comes from the queue depth of the storage interface, which is typically much larger than N_{\max} when multiple drives are used.

To put Equation 2 into context, consider a PCIe Gen 4.0 x16 link supported by modern GPUs. Then, $N_{\max} = 768$ due to the PCIe specification, and $W = 24,000$ MB/sec, for which we use an effective bandwidth rather than the theoretical value of 31,500 MB/sec. Now we suppose our external memory has $S = 100$ MIOPS (collectively,

if comprised of multiple devices) and $L = 16$ usec. These numbers are just for the sake of example. Then, Equation 2 becomes

$$T = \min\{100d, 48d, 24,000\}, \quad (4)$$

which is plotted as the bottom dotted line in Figure 4 (the other two lines will be explained in Section 3.3.2). We assume that the IOPS S and average latency L do not depend on the transfer size d , which is reasonable for flash-based external memory as long as the transfer size is under a certain size for which the device is optimized. For instance, typical SSDs are optimized for 4 kB access, and reading smaller bytes does not significantly increase the random read performance due to its internal page size and error correction size. Similar tendency can be observed for drives optimized for smaller sizes. Under this assumption, the plot linearly increases until it hits the bandwidth limit, and its slope s is given as

$$s = \min\left\{S, \frac{N_{\max}}{L}\right\}, \quad (5)$$

which is 48 in the above example.

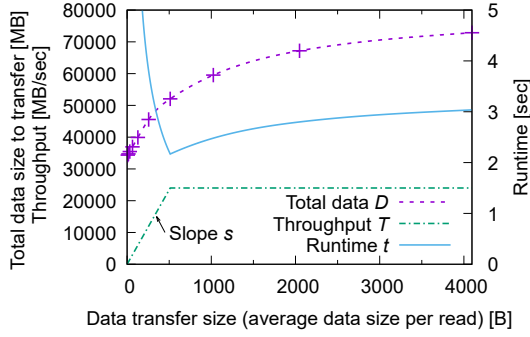


Figure 4: Runtime as a function of data transfer size.

3.3 Study of Existing Methods

In order to have a shorter runtime $t = D/T$, one wishes to decrease the total data size D (or equivalently, RAF) and increase the throughput T . The former can be done by using a smaller alignment size a while the latter by using a larger data transfer size d . We look at the state-of-the-art methods, EMOGI and BaM, in light of these objectives and see how they achieve optimal runtimes within their respective constraints. A PCIe Gen 4.0 x16 link is assumed.

3.3.1 EMOGI. EMOGI uses the host DRAM as external memory. It employs zero-copy access to the host DRAM, meaning that data is fetched from the host DRAM without copying it to the GPU memory. The data access is performed in the same way as to the GPU memory, and requests are issued at a multiple of 32 B up to the GPU’s hardware cache line size of 128 B [31]. Therefore, we have alignment size $a = 32$ B due to the GPU architecture, and the average data transfer size depends on the workload and how EMOGI cleverly issues 32 B reads so that the GPU merges them into a larger size when an edge sublist spans multiple of 32 B alignments [14]. From their evaluation [31], we assume the distribution of 32, 64, 94, 128-B accesses to be 20%, 20%, 20%, 40%, which translates to the average transfer size of $d_{\text{EMOGI}} = 0.2 \times 32 + 0.2 \times 64 + 0.2 \times 96 +$

$0.4 \times 128 = 89.6$ B. This is a conservative estimate (i.e., the worst case among the distributions reported in [31]), as 128-B reads are more dominant in many workloads.

As for the RAF, $a = 32$ B alignment is close to optimal as can be seen in Figure 3: smaller alignments will have a diminishing return.

Regarding the throughput, $d_{\text{EMOGI}} = 89.6$ B is sufficient in maximizing the throughput to saturate the PCIe bandwidth. Since the IOPS of the host DRAM-based external memory is excessively high, the slope s of the throughput in Equation 5 is limited by the latency, which is around 1.2 usec as seen from the GPU (measured in Section 4.2.2 as shown in Figure 9). This latency is still short enough because $s_{\text{EMOGI}} = (768/1.2) \times 89.6 = 57,344$ MB/s, which is greater than the PCIe bandwidth of $W = 24,000$ MB/sec.

3.3.2 BaM. BaM uses SSDs as external memory. As BaM implements a software cache on the GPU memory and reads data at a cache line granularity, we have $d = a$. In this case, we can plot both of D and T , and hence t as well, as a function of transfer size d . Figure 4 plots examples of them. The plot of the total data size D smoothly interpolates the data points taken from BFS for urand27 dataset. Note that it shows the raw data size in bytes along the linear horizontal axis in Figure 4 as opposed to Figure 3 showing RAF along the \log_2 axis. By dividing this D by the example throughput profile T described in Section 3.2, the solid line in Figure 4 shows the theoretically-expected runtime t of BFS algorithm for urand27 dataset for varying transfer sizes d . It is clear from this plot that the best (shortest) runtime is obtained at the minimum transfer size that still fully utilizes the bandwidth W . That is, the optimal transfer size d_{opt} satisfies $s d_{\text{opt}} = W$. Since BaM uses four of Intel P5800X SSDs totaling $S = 6$ MIOPS, and $s = S$ as this is storage access, the optimal size is given as $d_{\text{BaM}} = W/S = 24,000/6 \approx 4$ kB, which is indeed the cache line size mainly used in their evaluation.

Here, as seen from the denominator of the equation W/S , the IOPS is the limiting factor, requiring BaM to use a large data transfer size. This suggests that one might be able to achieve faster runtimes by using higher-IOPS memory devices and smaller transfer/alignment sizes.

3.4 Observations

From the analyses of the two methods above, we can see that EMOGI’s faster runtime than BaM can be primarily explained by the fact that EMOGI’s alignment of 32 B is smaller than that of BaM (typically 4 kB). Both methods maximize the throughput as $T = W$ in Equation 1, and therefore the difference comes from the total data size D , which prefers smaller alignments. Of course, there is a good reason why BaM chooses a large alignment size for the storage in use as explained in Section 3.3.2, but it also suggests a possibility of faster processing by using a smaller alignment size supported by high-IOPS memory devices.

In the meantime, Section 3.3.1 shows that EMOGI’s average transfer size is more than sufficient to fully utilize the PCIe bandwidth, indicating that we might be able to relax the specifications of external memory from those of the host DRAM. More specifically, in order to satisfy $s d_{\text{EMOGI}} \geq W$, we have

$$\min\left\{S, \frac{768}{L}\right\} \times 89.6 \geq 24,000. \quad (6)$$

This becomes $S \geq 268$ MIOPS and $L \leq 2.87$ usec. Therefore, an additional latency of a few microseconds, introduced by the CXL interface and the underlying memory devices, may be tolerated. While the IOPS requirement is rather high, it is feasible by bundling multiple high-IOPS (tens of MIOPS) devices together.

In summary, our observations are as follows. On the condition that we have sufficient random read performance,

Observation 1: A smaller address alignment size is better.

Observation 2: The allowable latency is a few microseconds.

3.5 Latency

So far, our latency L is limited by the allowable number N_{\max} of outstanding requests in the PCIe specification (256 for PCIe Gen 3.0 and 768 for Gen 4.0 and 5.0). However, there are also other factors having their own concurrency limits. Here we examine them and confirm that, currently, the strictest limit comes from PCIe.

3.5.1 Traversal Algorithm. Typically, BFS-like graph traversal is massively parallelizable. Table 2 shows how many vertices are being visited (i.e., frontier) at each depth of the search in BFS for urand27 dataset. Most depths have more than tens of thousands of vertices that can be processed independently, indicating that the algorithm itself does not limit concurrency. Some depths have smaller frontiers, but they contribute little to the overall runtime.

Table 2: Example numbers of vertices per traversal depth.

Depth	Number of vertices
1	31
2	984
3	31,252
4	995,253
5	28,130,066
6	104,931,066
7	129,075

3.5.2 GPU. There is an upper limit to the GPU concurrency, but it is much larger than $N_{\max} = 768$, and thus the GPU will not be a limiting factor. A group of GPU threads that execute the same instructions is called a *warp* [24], which is considered a unit of concurrency. The GPU we use has 3,072 warps. Fewer warps may actually run depending on the workload due to the limitations of other resources such as GPU registers. Yet, in our BFS execution, we find that 2,048 warps are running, which is still larger than N_{\max} .

3.5.3 CXL Interface. The CXL specification itself is unlikely to limit the number of outstanding reads, as 16 tag bits are available (65,536 outstanding requests) [5]. There is a possibility that CXL memory devices do not fully utilize them depending on their implementations, leaving a stricter latency allowance. Moreover, as the CXL data transfer size is 64 B, larger read requests from the GPU have to be split, consuming more tags. That said, our assumption is that CXL memory devices coming to the market in the near future will support a sufficient number of outstanding requests.

4 EVALUATION

As CXL-enabled flash memory devices are not available yet, we use two FPGA prototypes to support the analysis presented in Section 3. The first prototype, XLFDD, is a storage device equipped with low-latency flash memory reported elsewhere [38]. The second prototype is a DRAM-based CXL memory device with adjustable latency. The two prototypes respectively demonstrate **Observation 1** and **Observation 2** made in Section 3.4.

We use graph datasets listed in Table 1 including two synthetic graphs, uniform random graph (urand27) and Kronecker graph (kron27) having 2^{27} vertices [2], and a real-world graph Friendster [45]. We run BFS and SSSP as representative graph traversals involving fine-grained random access.

4.1 Evaluation on Low-Latency Flash Memory

We first show evaluation using XLFDD, a high-IOPS device supporting a small alignment of 16 B backed by low-latency flash memory. In support of **Observation 1**, we show that this small alignment enables much faster GPU graph processing than BaM with a 4 kB alignment, and demonstrate runtime performance close to using the host DRAM.

4.1.1 Implementation. Our implementation is conceptually similar to BaM in the sense that the GPU controls the storage devices directly without CPU intervention, but there are some differences coming from the use of XLFDDs instead of NVMe SSDs.

To explain XLFDD briefly, it is a PCIe-attached SSD equipped with low-latency flash chips with a latency of under 5 usec and with an FPGA implementing the storage controller. It implements a lightweight storage interface so that it can serve fine-grained accesses at up to 11 MIOPS. It supports a 16 B alignment, while the transfer size can be any multiple of 16 B up to 2 kB. This transfer size flexibility allows us to read a large edge sublist in one request without splitting it into the GPU cache line size of 128 B as would happen in the memory (host DRAM or CXL memory) access case. This makes the average transfer size d close to the average edge sublist size (256 B in urand27 and more in the other datasets), further relaxing the requirements for the external memory as $S \times 256 \geq 24,000$, leading to $S \geq 93.75$ MIOPS.

Table 3 summarizes our evaluation environment equipped with XLFDDs. With 16 drives, the system well supports the required random read speed of 93.75 MIOPS. To evaluate BaM, we replace XLFDDs with NVMe SSDs that collectively offer 6-MIOPS random read performance to match the number used in [33].

Table 3: System for evaluation on low-latency flash.

	Specifications
CPU	Intel Xeon Gold 6336Y (single socket)
DRAM	DDR4 3200 MHz 128 GB (16 GB \times 8 ch.)
GPU	NVIDIA RTX A5000, GDDR6 24GB, PCIe 4.0 x16
SSD	16 of XLFDD (PCIe 3.0 x4) 4 of KIOXIA FL6 800 GB NVMe (PCIe 4.0 x4)
OS	Ubuntu 20.04.3 LTS, Linux kernel 5.4.0
S/W	NVIDIA Driver 495.29.05, CUDA 11.5

As with BaM, we place submission queues (SQs) and data buffers in the base address register (BAR) section of the GPU memory in order to control storage devices directly from the GPU. Note that we do not have completion queues [42]. By memory-mapping BARs, the SQs and data buffers are accessible from XLFDDs.

Our graph processing software for XLFDD is similar to BaM. The major difference is that we do not implement software caches on the GPU memory, and instead directly access XLFDDs for simplicity. Because we use a much smaller alignment size than BaM’s, caches do not reduce the RAF much, and therefore this simplification has a minimal impact on performance.

4.1.2 Runtime Comparison. With this system, we show that a small alignment size leads to higher performance (**Observation 1**), and GPU graph processing speeds on low-latency flash memory can approach those on the host DRAM. We run our software on XLFDDs, BaM on the NVMe SSDs, and EMOGI on the host DRAM. Figure 5 shows the runtimes of BFS for urand27 dataset on XLFDD where we vary the address alignment size. The runtimes are normalized by that of EMOGI, and the normalized runtime of BaM with a 4 kB alignment is also shown for comparison. The plots demonstrate faster execution with smaller alignments, and at an alignment of 16 or 32 B, it approaches the speed on the host DRAM.

Figure 6 compares the normalized runtimes of XLFDD and BaM for all the pairs of the algorithms and datasets, where XLFDD uses a 16 B alignment. The runtimes of XLFDD are much closer to those of EMOGI (1.13 times longer on average, where the geometric mean is taken over all the six pairs) than those of BaM (2.76 times longer).

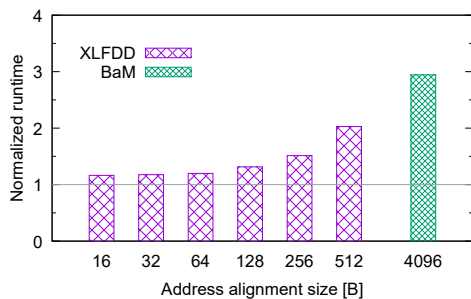


Figure 5: Runtimes of BFS for urand27 dataset on XLFDD with varying alignment sizes, along with the runtime of BaM, normalized by that of EMOGI.

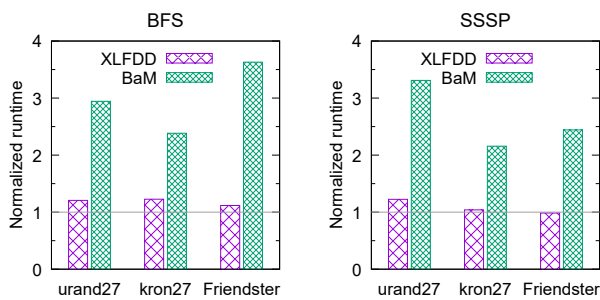


Figure 6: Runtimes of BFS (left) and SSSP (right) on XLFDD and BaM, normalized by those of EMOGI on the host DRAM.

4.2 Evaluation on CXL Memory

Next, we show evaluation using a DRAM-based CXL memory prototype with adjustable latency. It implements the CXL.mem protocol, allowing us to evaluate the GPU graph processing on CXL memory for the first time, and to confirm the permissible latency imposed by the number N_{\max} of outstanding requests of the PCIe link. In support of **Observation 2**, we show that GPU graph traversals on CXL memory with a latency of up to a few microsecond can be as fast as that on the host DRAM.

4.2.1 Implementation. We execute EMOGI on latency-adjustable CXL memory instead of on the host DRAM. We implement CXL memory based on Intel Agilex®7 FPGA as also used in other existing works [21, 41]. Figure 7 shows the block diagram. The CXL interface has two instances of CXL.mem each connecting to latency bridges that we designed to introduce additional latency to the onboard DRAM (see Appendix A for details). The behaviors of the latency bridges can be controlled by setting registers via CXL.io. Due to the limitation of the current FPGA board, the onboard DRAM can be accessed only through a single channel by interleaving through the bus matrix, which limits the throughput that this CXL memory prototype can support per device.

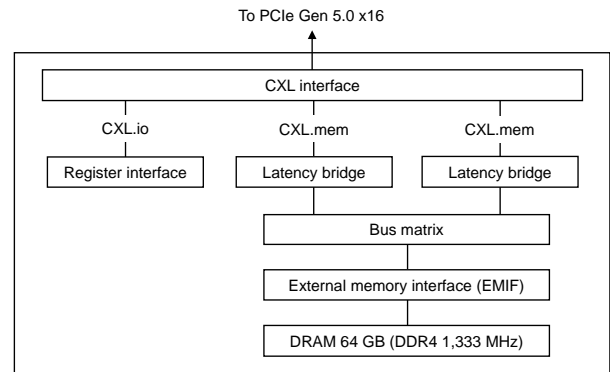


Figure 7: CXL memory prototype with adjustable latency.

Table 4 summarizes our evaluation system equipped with multiple of this CXL memory devices. Figure 8 illustrates the connectivity between the CPUs, GPU, and CXL memory devices. In our dual-socket system, the GPU is attached to CPU 1.

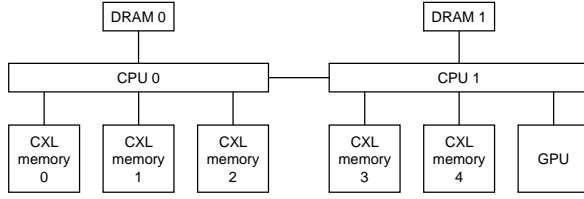
It is easy to set up CXL memory to be accessible from the GPU. One can use `set_mempolicy()` to specify the NUMA node ID corresponding to the CXL memory device. For instance, as explained in [31], `cudaMallocManaged()` can be used to allocate memory on the host DRAM for zero-copy access. The CXL equivalent can be done by calling `set_mempolicy()` before `cudaMallocManaged()`. Once done, the graph processing code of EMOGI works on the CXL memory without any modification. The GPU performs zero-copy access in the same way as does to the host DRAM, and the CPU translates it into CXL access.

4.2.2 System Performance Characterization. Before running GPU graph processing, we conduct some microbenchmarks to characterize the system performance in terms of latency, throughput, random read performance, and the number of outstanding requests.

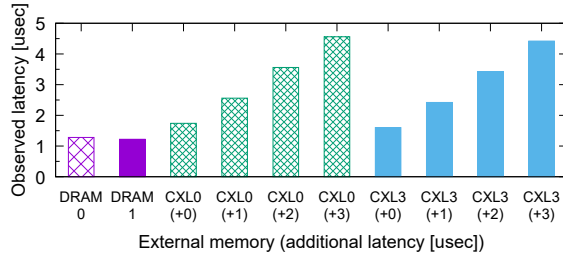
Table 4: System for evaluation on CXL memory.

Specifications	
CPU 0/1	Intel Sapphire Rapids* (dual socket)
DRAM 0	DDR5 4800 MHz 192 GB (32 GB × 6 ch.)
DRAM 1	DDR5 4800 MHz 32 GB (32 GB × 1 ch.)
GPU	NVIDIA RTX A5000, GDDR6 24 GB, PCIe 4.0 x16
CXL	5 of Intel Agilex®7 FPGA I-Series Dev. Kit
OS	Fedora 34, Linux kernel 5.4.0
S/W	NVIDIA Driver 530.30.02, CUDA 12.1

* Evaluation based on Intel reference designs and pre-production 4th Gen Intel Xeon Scalable processors.

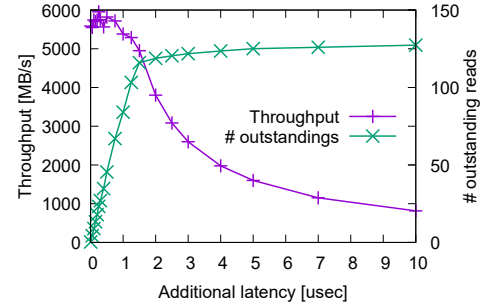
**Figure 8: Connectivity of CPUs, GPU, and CXL memory.**

First, we measure the latency introduced by the CXL memory by running pointer chasing on the GPU to access external memory (see Appendix B for details). The results are shown in Figure 9. For the CXL memory, we vary the additional latency as shown in the parentheses. The observed latency becomes longer as our FPGA latency bridge adds more latency as expected. The GPU sees a latency of around 1+ usec going through the PCIe link to the host DRAM as also reported in [31], and the CXL DRAM introduces an additional latency of 0.5 usec. Access to external memory devices connected to the same CPU as the GPU (DRAM 1 and CXL 3 as in Figure 8, which are solid-filled in Figure 9) sees marginally shorter latencies than their counterparts connected to the other CPU (DRAM 0 and CXL 0). Note that the latencies reported here are those observed from the GPU, and therefore they are longer than those reported in the literature studying CXL memory access from the CPU [23, 29].

**Figure 9: Measured latency of host DRAM and CXL memory as seen from the GPU.**

Next, we have the CPU (not the GPU) issue random read requests to the CXL memory prototype using the CXL access size of $d_{CXL} = 64$ B, and plot the observed throughput T_{CXL} for varying latency

as shown in Figure 10. We use the subscript CXL to clarify that we are referring to the CXL memory characteristics rather than the PCIe link between the CPU and GPU. From the plot we can see that the throughput is capped at around 5,700 MB/sec due to the single-channel DRAM as mentioned above. The decrease in the throughput for longer latency indicates it is limited by the maximum number of outstanding requests of the CXL prototype, although the CXL specification itself permits 65536 of them as mentioned in Section 3.5.3. From Equation 3, the number N_{CXL} of concurrent requests for a given latency L_{CXL} can be computed as $N_{CXL} = T_{CXL}L_{CXL}/d_{CXL}$, which is also plotted in the same figure. This implies that the maximum number of outstanding requests that the current Intel Agilex®7 FPGA can handle is 128. Because a 128 B or 96 B read from the GPU through PCIe is split into two 64 B reads at the CXL level, the number of requests for the CXL memory can double. Thus, our CXL memory prototype can handle 64 (= 128/2) outstanding requests from the GPUs. While this number is a current limitation that we expect to be lifted in the near future, in order to use this prototype to test the scenario where the concurrency bottleneck is in the PCIe link to the GPU, we downgrade the PCIe link to Gen 3.0 and use five of the CXL memory devices (which is the maximum number of devices we are able to operate in the server), such that the maximum number of outstanding requests that the CXL memory devices can collectively handle, which is 320 (= 64 × 5), is larger than that of PCIe Gen 3.0 ($N_{max} = 256$).

**Figure 10: Bandwidth and the number of outstanding reads of the CXL memory prototype for varying additional latency.**

With PCIe Gen 3.0 x16 link for the GPU, the effective bandwidth is halved as $W = 12,000$ MB/sec, and the requirements for external memory becomes $S = W/d_{EMOGI} = 12,000/89.6 = 134$ MIOPS and $L = N_{max} d_{EMOGI}/W = 256 \times 89.6/12,000 = 1.91$ usec. The halved bandwidth can be saturated by five CXL memory devices when the additional latency is less than 3 usec at which the per-device throughput is around 2,500 MB/sec as shown in Figure 10.

4.2.3 Runtime Comparison. Here we show that GPU graph processing on CXL memory is as fast as that on the host DRAM, as long as the CXL memory latency is up to a few microseconds (**Observation 2**). We execute BFS and SSSP on the GPU using either the host DRAM or CXL memory as external memory over PCIe Gen 3.0 x16 link to the GPU. For each algorithm, the same EMOGI code is used for both the host DRAM and CXL memory. We vary the additional latency of the CXL memory from 0 to 3 usec. For each

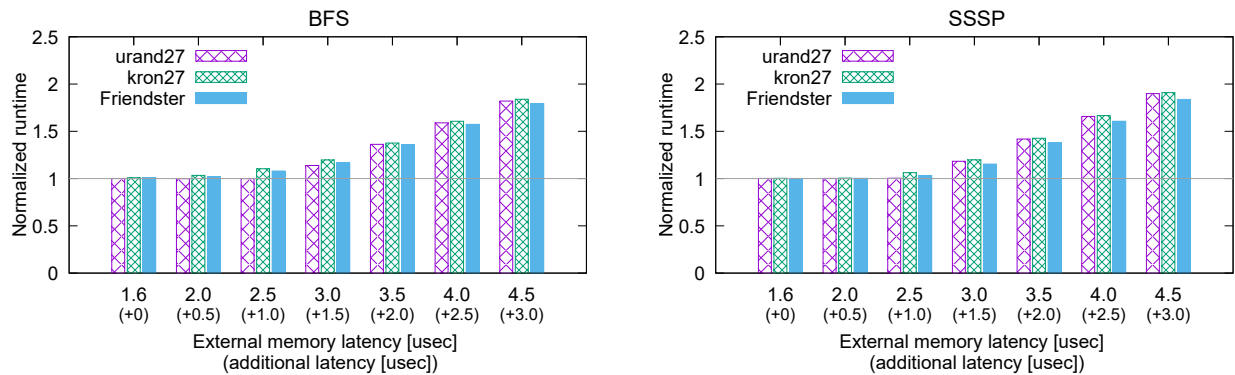


Figure 11: Runtimes of BFS (left) and SSSP (right) on CXL memory with varying latency, normalized by those on host DRAM.

graph data set, the runtimes on the CXL memory are normalized by that using the host DRAM, and plotted in Figure 11. The latencies written above the parenthesized additional latencies are those seen from the GPU derived according to Figure 9. As long as the CXL memory latency from the GPU is under around 2 usec (≈ 1.91 usec as calculated in Section 4.2.2), we see that the runtime on CXL memory is almost identical to that on the host DRAM as expected.

5 DISCUSSION

This section discusses limitations to our work and points not considered in the paper, all of which present future research avenues.

Prototype limitations: Our evaluation using the two prototypes has both demonstrated runtime performance close to using the host DRAM in GPU graph processing on microsecond-latency external memory. However, it has fallen short of full demonstration of our target: the one involving both the CXL interface and real microsecond-latency memory devices. The limitations of our work come from our preliminary CXL memory implementation. It is emulated memory with longer latency, which does not necessarily model all the aspects of real devices. Nonetheless, we believe our flash-based (although non-CXL) prototype complements it, so that our evaluation using both prototypes jointly provides insight into how a given system may achieve host DRAM-like performance. Even though the PCIe generations each double the bandwidth, the GPU and memory performance also increases accordingly. Thus, it is likely that the PCIe link to the GPU will continue to be the bottleneck, and our analysis will apply in the foreseeable future.

Our analysis indicates that the full demonstration mentioned above would permit a latency of around 3 usec as described in Section 3.4. While this is still shorter than the low-latency flash memory currently available, we believe this requirement is within reach considering the technological advancements in memory devices as well as in CXL memory implementations.

Read-only workloads: The graph processing workloads evaluated in this paper are all read-only. While CXL is a cache-coherent protocol, the coherency overhead should be minimal for read-only workloads, if any. For workloads involving write access, there will be a number of additional factors to be considered, including cache coherency mentioned above and write characteristics of flash memory, all of which may have dependencies on the address alignment

size a and data transfer size d . These factors can translate to performance impacts. Furthermore, additional care will have to be taken if memory persistency needs to be ensured.

Other system configurations: The premise of our analysis and evaluation is that the GPU onboard memory is limited and benefits from external memory through the PCIe link. This does not always hold: one can opt to use GPUs having large memory (e.g., 80 GB [6]) or bundle multiple of them to create an even larger pool of GPU memory. Moreover, some emerging architectures integrate a CPU and GPU on the same chip, bringing the host DRAM closer to the GPU [1, 7]. In both cases, HBM (High Bandwidth Memory) enables a much higher throughput than what a PCIe link offers. If performance is more heavily weighted than cost, these system configurations can be compelling options. In the meantime, our projection is that PCIe-attached GPUs with limited memory will continue to constitute cost-effective options, and we believe flash-based CXL memory can make those options even more appealing.

Currently, CXL memory access from the GPU goes through the CPU. The GPU does not use the CXL protocol, and issues requests in the same way as when accessing the host DRAM, and the CPU translates them into CXL access. However, future GPUs may implement the CXL interface to directly communicate with CXL memory. Still, our analysis will remain valid so far as the PCIe link to the GPU continues to be the bottleneck. As the direct communication will reduce the CXL memory latency seen from the GPU, it will likely become easier to achieve a latency of a few microseconds.

Other graph formats and preprocessing: Our evaluation has used a BaM-like implementation for XLFDD, and EMOGI for CXL memory, both of which perform fine-grained access to external memory on demand. We have used them because they achieve state-of-the-art runtime performance. They are also beneficial in that the GPU can directly take an input graph in the standard CSR format without preprocessing. However, fine-grained access implies a small average data transfer size d over the PCIe link. Although a larger d will relax the latency and IOPS requirements for external memory, we cannot arbitrarily increase d as it depends on the input graph: increasing d beyond the average edge sublist size will increase the RAF, leading to a negative performance impact. Therefore, in order to increase d further, it would be interesting to consider tailored graph formats and preprocessing such as [13, 35, 36].

6 RELATED WORK

CPU graph processing: When graph data fits in the host DRAM, in-memory graph processing methods like Galois [32] and GAP [2] can be used. When it does not fit in the DRAM, one option is distributed processing [27], but communication overheads limit the performance [8, 30]. For this reason, single-node approaches utilizing storage devices as external memory have been proposed [16, 17, 20, 25, 26, 34, 47]. Graphene [25] achieves excellent performance close to in-memory solutions for algorithms mainly involving sequential access such as PageRank, but it is significantly slower if random access is required like in BFS. Graph algorithms involving random access has been shown to approach in-memory speeds if executed on low-latency flash-based storage by accessing it using lightweight context switching to hide latency [42]. In this paper we address random access graph workloads on the GPU using external memory, and find quite different requirements than the CPU case.

GPU graph processing on the host DRAM: It is natural to consider taking advantage of massive compute resources of the GPU for graph processing. As the GPU onboard memory is even more limited, many prior works propose to place graph data on the host DRAM [9–11, 18, 22] (in contrast to the CPU case, the host DRAM is viewed as external memory from the GPU). These methods are based on a unified virtual memory (UVM) approach where portions of the host DRAM are copied to the GPU memory via paging at a 4 kB granularity [15]. EMOGI instead uses zero-copy access and has shown that this fine-grained direct access significantly reduces the RAF compared with the UVM approach [31]. This paper has shown that EMOGI stays as performant even if the external memory latency is longer than the host DRAM, up to a few microseconds.

GPU graph processing on storage: BaM introduced a first GPU-centric storage access method that does not involve CPU intervention [33]. While there are several prior works in GPU-centric approaches [28, 37, 39, 40, 43], they rely on the CPU to handle storage access and use the GPU memory as a staging buffer for their data transfer. BaM has shown that it achieves competitive runtimes with EMOGI when the EMOGI’s runtimes include the time for loading graph data from SSDs. This paper has shown that, by using external memory based on microsecond-latency flash memory, we can achieve even faster runtimes so that they are close to those of EMOGI even if we exclude EMOGI’s file loading time.

CXL analysis and evaluation: CXL is an emerging standard that is attracting attention not only from industry but also from research communities. Analysis and evaluation of CXL-enabled systems are being conducted ranging from memory pooling in general [12, 23, 41, 44, 46], to more specific applications such as machine learning [19] and in-memory databases [21]. CXL studies involving accelerators such as GPU and FPGA are appearing [3, 19]. Our work complements these studies and deals with GPU graph processing on CXL memory for the first time.

7 CONCLUSION

We have presented analysis and evaluation of GPU graph traversal using CXL-based external memory. Given the nature of the workload where on-demand, fine-grained random reads are bottlenecked by the PCIe link to the GPU, we note that a small address alignment of around 32 B, along with appropriately-sized data transfer close

to the average edge sublist size of a few hundred bytes, will lead to an optimal runtime. This translates into the requirements for external memory, which are random read performance of a few hundred MIOPS and a latency of a few microseconds, suggesting the possibility that CXL memory with longer latency, including that equipped with low-latency flash memory, may be used as external memory to achieve performance comparable to the host DRAM.

To support these observations, we have conducted evaluation using two FPGA-based external memory prototypes, one is a storage device with low-latency flash memory and the other DRAM-based CXL memory with adjustable latency, and we have demonstrated GPU graph processing speeds close to using the host DRAM when the external memory latency is under a few microseconds.

While our evaluation is limited by the current availability of CXL devices, we believe it provides first preliminary characterizations of GPU access to CXL memory, which we hope leads to insights into how cost-effective systems may be constructed potentially by incorporating flash-based CXL memory.

A LATENCY BRIDGE DESIGN

The latency bridge described in Section 4.2.1 is implemented as shown in Figure 12. We add a time stamp to an incoming read request, read data from the DRAM, and push it to a FIFO along with the time stamp. When the current time becomes greater than the time stamp of the FIFO head by a specified additional latency, the data is popped and sent to the CPU through the CXL interface. As the CXL interface of Intel Agilex®7 FPGA processes requests in order at the time of this work, a FIFO is sufficient, but a slightly more involved design would be required to support out-of-order access.

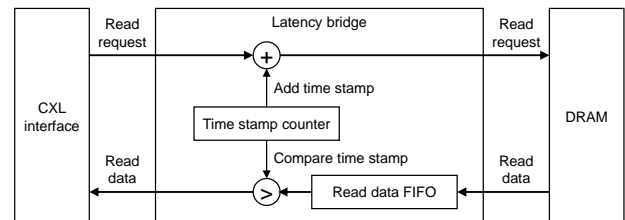


Figure 12: Block diagram of the latency bridge.

B POINTER CHASING FROM THE GPU

We perform pointer chasing to measure the latency of CXL memory (and the host DRAM) from the GPU as described in Section 4.2.2. In preparation, we allocate a 16-GB block of CXL memory and fill it with 134 million 128-B indices (or pointers) each pointing to the next address to look at. We run a single GPU warp [24] to chase them: it reads the first pointer, then reads the next pointer stored at the address pointed to by the first pointer, and so on. The pointers are set in such a way that the GPU has to move randomly in the 16-GB space. The 32 GPU threads in a warp each fetch 4 B of a 128-B pointer and synchronize before reading the next pointer. The runtime of this operation is determined by the memory latency as the next pointer is only available after reading the current pointer.

REFERENCES

- [1] Advanced Micro Devices, Inc. 2023. AMD Expands Leadership Data Center Portfolio with New EPYC CPUs and Shares Details on Next-Generation AMD Instinct Accelerator and Software Enablement for Generative AI. <https://www.amd.com/en/newsroom/press-releases/2023-6-13-amd-expands-leadership-data-center-portfolio-with-.html>.
- [2] Scott Beamer, Krste Asanović, and David Patterson. 2015. The GAP benchmark suite. *arXiv preprint arXiv:1508.03619* (2015).
- [3] Anthony M Cabrera, Aaron R Young, and Jeffrey S Vetter. 2022. Design and Analysis of CXL Performance Models for Tightly-Coupled Heterogeneous Computing. In *the 1st International Workshop on Extreme Heterogeneity Solutions (ExHET)*. Article 1.
- [4] The CXL Consortium. [n. d.]. Compute Express Link™. <https://www.computeexpresslink.org/>.
- [5] Intel Corporation. 2023. Compute Express Link (CXL)-Cache/Mem Protocol Interface (CPI). https://cdrdv2-public.intel.com/644330/644330_CPIspecification_Rev1p0.pdf.
- [6] NVIDIA Corporation. 2023. NVIDIA A100 Tensor Core GPU. <https://www.nvidia.com/en-us/data-center/a100/>.
- [7] NVIDIA Corporation. 2023. NVIDIA Grace Hopper Superchip. <https://www.nvidia.com/en-us/data-center/grace-hopper-superchip/>.
- [8] Roshan Dathathri, Gurbinder Gill, Loc Hoang, Hoang-Vu Dang, Alex Brooks, Nikoli Dryden, Marc Snir, and Keshav Pingali. 2018. Gluon: A communication-optimizing substrate for distributed heterogeneous graph analytics. In *Proceedings of the 39th ACM SIGPLAN conference on programming language design and implementation*. 752–768.
- [9] H Carter Edwards, Christian R Trott, and Daniel Sunderland. 2014. Kokkos: Enabling manycore performance portability through polymorphic memory access patterns. *Journal of parallel and distributed computing* 74, 12 (2014), 3202–3216.
- [10] Prasun Gera, Hyojong Kim, Piyush Sao, Hyesoon Kim, and David Bader. 2020. Traversing large graphs on GPUs with unified memory. *Proceedings of the VLDB Endowment* 13, 7 (2020), 1119–1133.
- [11] Juan Gómez-Luna, Izzat El Hajj, Li-Wen Chang, Victor García-Floreszc, Simon García De Gonzalo, Thomas B Jablin, Antonio J Pena, and Wen-mei Hwu. 2017. Chai: Collaborative heterogeneous applications for integrated-architectures. In *2017 IEEE International Symposium on Performance Analysis of Systems and Software (ISPASS)*. IEEE, 43–54.
- [12] Donghyun Gouk, Sangwon Lee, Miryeong Kwon, and Myoungsoo Jung. 2022. Direct Access, High-Performance Memory Disaggregation with DirectCXL. In *the 2022 USENIX Annual Technical Conference*. Carlsbad, CA, USA.
- [13] Wei Han, Daniel Mawhirter, Bo Wu, and Matthew Buland. 2017. Graphie: Large-Scale Asynchronous Graph Traversals on Just a GPU. In *26th International Conference on Parallel Architectures and Compilation Techniques (PACT)*. IEEE, Portland, OR, USA, 31–46. <https://doi.org/10.1109/PACT.2017.41>
- [14] Mark Harris. 2013. How to Access Global Memory Efficiently in CUDA C/C++ Kernels. <https://developer.nvidia.com/blog/how-access-global-memory-efficiently-cuda-c-kernels/>.
- [15] Mark Harris. 2017. Unified Memory for CUDA Beginners. <https://developer.nvidia.com/blog/unified-memory-cuda-beginners/>.
- [16] Sang-Woo Jun, Andy Wright, Sizhuo Zhang, Shuotao Xu, et al. 2017. BigSparse: High-performance external graph analytics. *arXiv preprint arXiv:1710.07736* (2017).
- [17] Sang-Woo Jun, Andy Wright, Sizhuo Zhang, Shuotao Xu, et al. 2018. GrafBoost: Using accelerated flash storage for external graph analytics. In *2018 ACM/IEEE 45th Annual International Symposium on Computer Architecture (ISCA)*. IEEE, 411–424.
- [18] Hyojong Kim, Jaewoong Sim, Prasun Gera, Ramyad Hadidi, and Hyesoon Kim. 2020. Batch-aware unified memory management in GPUs for irregular workloads. In *Proceedings of the Twenty-Fifth International Conference on Architectural Support for Programming Languages and Operating Systems*. 1357–1370.
- [19] Miryeong Kwon, Junhyeok Jang, Hanjin Choi, Sangwon Lee, and Myoungsoo Jung. 2023. Failure Tolerant Training with Persistent Memory Disaggregation over CXL. *IEEE Micro* 43, 2 (jan 2023), 66–75. <https://doi.org/10.1109/MM.2023.3237548>
- [20] Aapo Kyrola, Guy Blelloch, and Carlos Guestrin. 2012. GraphChi: Large-Scale Graph Computation on Just a PC. In *10th USENIX Symposium on Operating Systems Design and Implementation (OSDI 12)*. 31–46.
- [21] Donghun Lee, Thomas Willhalm, Minseon Ahn, Suprasad Mutalik Desai, Daniel Booss, Navneet Singh, Daniel Ritter, Jungmin Kim, and Oliver Rebolhos. 2023. Elastic Use of Far Memory for In-Memory Database Management Systems. In *Proceedings of the 19th International Workshop on Data Management on New Hardware (DaMoN)*. 35–43.
- [22] Chen Li, Rachata Ausavarunirun, Christopher J Roszbach, Youtao Zhang, Onur Mutlu, Yang Guo, and Jun Yang. 2019. A framework for memory oversubscription management in graphics processing units. In *Proceedings of the Twenty-Fourth International Conference on Architectural Support for Programming Languages and Operating Systems*. 49–63.
- [23] Huaicheng Li, Daniel S. Berger, Lisa Hsu, Daniel Ernst, Pantea Zardoshti, Stanko Novakovic, Monish Shah, Samir Rajadnya, Scott Lee, Ishwar Agarwal, Mark D. Hill, Marcus Fontoura, and Ricardo Bianchini. 2023. Pond: CXL-Based Memory Pooling Systems for Cloud Platforms. In *Proceedings of the 28th ACM International Conference on Architectural Support for Programming Languages and Operating Systems (ASPLOS)*, Vol. 2. Vancouver, BC Canada, 574–587.
- [24] Yuan Lin and Vinod Grover. 2018. Using CUDA Warp-Level Primitives. <https://developer.nvidia.com/blog/using-cuda-warp-level-primitives/>.
- [25] Hang Liu and H Howie Huang. 2017. Graphene: Fine-Grained IO Management for Graph Computing. In *15th USENIX Conference on File and Storage Technologies (FAST 17)*. 285–300.
- [26] Steffen Maass, Changwoo Min, Sanidhya Kashyap, Woonhak Kang, Mohan Kumar, and Taesoo Kim. 2017. Mosaic: Processing a trillion-edge graph on a single machine. In *Proceedings of the Twelfth European Conference on Computer Systems*. 527–543.
- [27] Grzegorz Malewicz, Matthew H Austern, Aart JC Bik, James C Dehnert, Ilan Horn, Naty Leiser, and Grzegorz Czajkowski. 2010. Pregel: a system for large-scale graph processing. In *Proceedings of the 2010 ACM SIGMOD International Conference on Management of data*. 135–146.
- [28] Pak Markthub, Mehmet E Belviranlı, Seyong Lee, Jeffrey S Vetter, and Satoshi Matsuoka. 2018. DRAGON: breaking GPU memory capacity limits with direct NVM access. In *SC18: International Conference for High Performance Computing, Networking, Storage and Analysis*. IEEE, 414–426.
- [29] Hasan Al Maruf, Hao Wang, Abhishek Dhanotia, Johannes Weiner, Niket Agarwal, Pallab Bhattacharya, Chris Petersen, Mosharaf Chowdhury, Shobhit Kanaujia, and Prakash Chauhan. 2023. TPP: Transparent Page Placement for CXL-Enabled Tiered-Memory. In *Proceedings of the 28th ACM International Conference on Architectural Support for Programming Languages and Operating Systems (ASPLOS)*, Vol. 3. Vancouver, BC Canada, 742–755.
- [30] Frank McSherry, Michael Isard, and Derek G Murray. 2015. Scalability! but at what COST?. In *15th Workshop on Hot Topics in Operating Systems (HotOS XV)*.
- [31] Seung Won Min, Vikram Sharma Mailthody, Zaid Qureshi, Jinjun Xiong, Eiman Ebrahimi, and Wen mei W. Hwu. 2020. EMOGI: Efficient Memory-access for Out-of-memory Graph-traversal In GPUs. *Proc. VLDB Endow.* 14 (2020), 114–127.
- [32] Donald Nguyen, Andrew Lenharth, and Keshav Pingali. 2013. A lightweight infrastructure for graph analytics. In *Proceedings of the twenty-fourth ACM symposium on operating systems principles*. 456–471.
- [33] Zaid Qureshi, Vikram Sharma Mailthody, Isaac Gelado, Seung Won Min, Amna Masood, Jeongmin Park, Jinjun Xiong, CJ Newburn, Dmitri Vainbrand, I Chung, et al. 2022. GPU-Initiated On-Demand High-Throughput Storage Access in the BaM System Architecture. In *Proceedings of the 28th ACM International Conference on Architectural Support for Programming Languages and Operating Systems (ASPLOS)*, Vol. 2. 325–339.
- [34] Amitabha Roy, Ivo Mihailovic, and Willy Zwaenepoel. 2013. X-stream: Edge-centric graph processing using streaming partitions. In *Proceedings of the Twenty-Fourth ACM Symposium on Operating Systems Principles*. 472–488.
- [35] Amir Hossein Nodehi Sabet, Zhijia Zhao, and Rajiv Gupta. 2020. Subway: Minimizing Data Transfer during out-of-GPU-Memory Graph Processing. In *15th European Conference on Computer Systems (EuroSys '20)*. Heraklion, Greece, Article 12:1–16.
- [36] Dipanjan Sengupta, Shuaiwen Leon Song, Kapil Agarwal, and Karsten Schwan. 2015. GraphReduce: Processing Large-Scale Graphs on Accelerator-Based Systems. In *International Conference for High Performance Computing, Networking, Storage and Analysis (SC '15)*. Austin, TX, USA, Article 28:1–12. <https://doi.org/10.1145/2807591.2807655>
- [37] Sagi Shahar, Shai Bergman, and Mark Silberstein. 2016. ActivePointers: a case for software address translation on GPUs. *ACM SIGARCH Computer Architecture News* 44, 3 (2016), 596–608.
- [38] Tatsuo Shiozawa, Hirotsugu Kajihara, Tatsuro Endo, and Kazuhiro Hiwada. 2020. Emerging Usage and Evaluation of Low Latency FLASH. In *2020 IEEE International Memory Workshop (IMW)*. IEEE, 1–4.
- [39] Mark Silberstein, Bryan Ford, Idit Keidar, and Emmett Witchel. 2014. GPUfs: Integrating a file system with GPUs. *ACM Transactions on Computer Systems (TOCS)* 32, 1 (2014), 1–31.
- [40] Mark Silberstein, Sangman Kim, Seonggu Huh, Xinya Zhang, Yige Hu, Amir Wated, and Emmett Witchel. 2016. GPUUnet: Networking abstractions for GPU programs. *ACM Transactions on Computer Systems (TOCS)* 34, 3 (2016), 1–31.
- [41] Yan Sun, Yifan Yuan, Zeduo Yu, Reese Kuper, Ipoom Jeong, and Ren Wang Nam Sung Kim. 2023. Demystifying CXL Memory with Genuine CXL-Ready Systems and Devices. *arXiv preprint arXiv:2303.15375* (2023).
- [42] Tomoya Suzuki, Kazuhiro Hiwada, Hirotsugu Kajihara, Shintaro Sano, Shuou Nomura, and Tatsuo Shiozawa. 2021. Approaching DRAM Performance by Using Microsecond-Latency Flash Memory for Small-Sized Random Read Accesses: A New Access Method and Its Graph Applications. *Proc. VLDB Endow.* 14, 8 (apr 2021), 1311–1324. <https://doi.org/10.14778/3457390.3457397>
- [43] Ján Veselý, Arkaprava Basu, Abhishek Bhattacharjee, Gabriel H Loh, Mark Oskin, and Steven K Reinhardt. 2018. Generic system calls for GPUs. In *2018 ACM/IEEE 45th Annual International Symposium on Computer Architecture (ISCA)*. IEEE,

- 843–856.
- [44] Jacob Wahlgren, Maya Gokhale, and Ivy Peng. 2022. Evaluating Emerging CXL-enabled Memory Pooling for HPC Systems. In *SC Workshop on Memory Centric High Performance Computing (MCHPC'22)*. Dallas, TX, USA.
- [45] Jaewon Yang and Jure Leskovec. 2012. Defining and evaluating network communities based on ground-truth. In *Proceedings of the ACM SIGKDD Workshop on Mining Data Semantics*. 1–8.
- [46] Yiwei Yang, Pooneh Safayanikoo, Jiacheng Ma, Tanvir Ahmed Khan, and Andrew Quinn. 2023. CXLMemSim: A pure software simulated CXL.mem for performance characterization. *arXiv preprint arXiv:2303.06153* (2023).
- [47] Da Zheng, Disa Mhembere, Randal Burns, Joshua Vogelstein, Carey E Priebe, and Alexander S Szalay. 2015. FlashGraph: Processing Billion-Node Graphs on an Array of Commodity SSDs. In *13th USENIX Conference on File and Storage Technologies (FAST 15)*. 45–58.